Transient Variability In Vapor Intrusion And The Factors That Influence It

Jonathan G. V. Ström,† Yijun Yao,‡ and Eric M. Suuberg*,†

†*Brown University, School of Engineering, Providence, RI, USA*

‡*Zhejiang University, Hangzhou, China*

E-mail: eric_suuberg@brown.edu

Abstract

Temporal variability in indoor air contaminant concentrations at vapor intrusion (VI) sites has been a concern for some time. We consider the source of the variability at VI sites located near Hill Air Force Base and Naval Air Station North Island using statistical analysis methods and three-dimensional subsurface computational fluid dynamics modeling. The results suggest that an order of magnitude variation in indoor air contaminant concentrations may be expected at "normal" VI sites where preferential pathways do not play a role, whereas three or more orders of magnitude can be observed at sites characterized by preferential pathways. A CFD modeling sensitivity analysis reveals that it is not only the presence of contaminant vapor in a preferential pathway that is required to see large observed variations, but there must also exist a permeable region beneath the structure. Large temporal fluctuations in indoor air contaminant concentrations may be observed where no preferential pathways exist, but this requires a particular combination of large fluctuations in pressure driving force and high soil permeability.

Introduction

Long term vapor intrusion (VI) studies in both residential and larger commercial structures have raised concerns regarding significant observed transient behavior in indoor air contaminant concentrations.[1–6] VI involves the migration of volatilizing contaminants from soil, groundwater or other subsurface sources into overlying structures. VI has been a recognized problem for some time, but many aspects remain poorly understood, particularly with respect to the causes of large temporal transients in indoor air concentrations. There is uncertainty within the VI community regarding how to best develop sampling strategies to address this problem.[1,3,7]

Results from a house operated by Arizona State University (ASU) near Hill AFB in Utah, an EPA experimental house in Indianapolis, IN and a large warehouse at the Naval Air Station (NAS) North Island, CA have all shown significant transient variations in indoor air contaminant concentrations. All were outfitted with sampling and monitoring equipment that allowed tracking temporal variation in indoor air contaminant concentrations on time scales of hours. All have shown that these concentrations varied significantly with time - orders of magnitude on the timescale of a day or days.[5,8,9]

In one instance the source of the variation was clearly established during the study; at the ASU house a field drain pipe (or "land drain"), which connected to a sewer system, was discovered beneath the house, and careful isolation of this source led to a clear conclusion that this preferential pathway significantly contributed to observed indoor air contaminant levels and their fluctuations.[9,10] While in this case the issue of a contribution from a preferential pathway was clearly resolved, what it left open was a question of whether existence of such a preferential pathway to an area beneath a structure would always be expected to lead to large fluctuations in indoor air contaminant concentrations.

Similarly, a sewer pipe has recently been suggested to be a source of the contaminants found in the EPA Indianapolis house.[11] That site was also characterized by large indoor air contaminant concentration fluctuations. Sewer lines have been generally implicated as VI source at several sites to date.[11–14] A Danish study estimates that roughly 20% of all VI sites in central Denmark involve significant sewer VI pathways.[?] Thus while the consideration of a role of possible sewer or other preferential pathways is now part of normal good practice in VI site investigation, it is still not known whether the existence of such pathways automatically means that large temporal fluctuations are necessarily to be expected. In some of these cases,[12,14] the sewer provided a pathway for direct entry of contaminant into the living space. While potentially important in many cases, this scenario is not further considered here, where the focus is on pathways that deliver contaminant to the soil beneath a structure.

It is, however, now known that even absent a preferential pathway, there may be significant transient variation in indoor air contaminant concentrations at VI sites.[2,4,15] One example is a site at NAS North Island at which no preferential pathways have been identified. Instead, a building at this site is characterized by significant variations in indoor-outdoor pressure differential.[5] It is believed that this is the origin of the fluctuations at that site.

This paper investigates the sources of the temporal variation in indoor air contaminant concentrations in both the presence and absence of in soil preferential pathways. In this work, the latter scenarios are referred to as "normal" VI scenarios, in which there is typically a groundwater source of the contaminant. Specifically, we pose the question of just how much variation in indoor air contaminant concentration may be expected at such normal VI sites vs. those characterized by preferential pathways. The conditions required for preferential pathways to be significant contributors to temporal variations in indoor air contaminant concentrations are also explored, and the consequences for sampling strategies are also discussed.

Methods

Statistical Analysis Of Field Data

To begin to characterize transient behavior in indoor air contaminant concentrations, actual datasets are analyzed to establish common levels of variability at VI sites. For this purpose, the datasets from the ASU house in Utah, the EPA Indianapolis site and North Island NAS were chosen for analysis. This paper relies on statistical analysis of published field data, and readers are referred to the original works for details regarding data acquisition.[3,5,8,9,16]

The ASU house and data were obtained over a period of a few years. During part of this time, controlled pressure method (CPM) tests were being conducted, in which the house was underpressurized to an extent greater than that characterizing "normal" operation. This caused greater than normal advective flow from the subsurface into the house, thus increasing VI potential.[6,8,17] This period of CPM testing is considered separately from the otherwise "natural" VI conditions in the analysis. Likewise, the existence of a preferential pathway at the ASU house needs to be considered in examining the dataset, noting that during some of the testing, this pathway was deliberately cut off, resulting in what we have termed "normal" VI conditions in which the main source of contaminant was believed to be groundwater.

The NAS North Island dataset has not (as far as is known) been influenced by a preferential pathway, but the structure there was subject to large internal pressure fluctuations, much more extensive than those typically recorded at the ASU house during normal operations. Additionally, the underlying soil at NAS North Island is sandy and more permeable than that at the ASU site, which, as will be shown, contributes to the indoor air contaminant concentrations being more sensitive to pressure fluctuations.[5]

Likewise, the Indianapolis site investigation spanned over a number of years and periodically included the testing of a sub-slab depressurziation system (SSD). The goal of which is to mitigate the VI risk by drastically depressurizing the sub-slab area underneath the house, preventing the contaminants from entering the structure above, and therefore only the period before the installation of this system was considered in the analysis. It is likely a sewer line beneath the structure acted as a preferential pathway,[11] however at no point was this PP removed, making it difficult to assess how significant the PP was at this site, regardless it is of interest to analyze this site due to its wealth of data.

The typical variation in indoor air contaminant concentrations with time will first be considered below in the case of the ASU house during "natural", (i.e. non-CPM conditions), in the case of the NAS North Island site over the entire available dataset, and for the Indianapolis case we consider the variations before the installation of the SSD system. The deviations from the mean TCE (Chloroform and PCE at the Indianapolis site) in indoor air concentration, as well as the indoor-outdoor pressure differential associated with these concentration fluctuations, were examined, and both univariate and bivariate kernel density estimations (KDE) were constructed. KDE is a technique that estimates the probability distribution of a random variable(s) by using multiple kernels, or weighting functions, and in this case, Gaussian kernels are used to create the KDEs. This means that it is presumed that the variables of interest (i.e., indoor air contaminant concentrations and indoor-outdoor pressure differentials, as sampled) are normally distributed around mean values (that there is statistical fluctuation associated with each sampling event). In this instance, the scipy statistical package was used to construct the KDEs, assuming a bandwidth parameter determined by Scott's rule. The distributions of the individual parameters and the relationship between them will be examined using the KDE method.

Modeling Work

In addition to examining the actual field data, a previously described three -dimensional computational fluid dynamics model of a generic VI impacted house was used to elucidate certain aspects of the processes. This model was implemented in a finite element solver, COMSOL Multiphysics. In the present work, there has been an addition of a preferential pathway to the "standard" model that has been described before in publications by this group.[18–20] In this modeling work, only the vadose zone soil domain is directly modeled.

The modeled structure is assumed to have a 10x10 m foundation footprint, with the bottom of the foundation slab lying 1 m below ground surface (bgs), simulating a house with a basement. The indoor air space is modeled as a continuously stirred tank (CST)[1] and all of the contaminant entering the house is assumed to enter with soil gas through a 1 cm wide crack located between the foundation walls and the foundation slab that spans the perimeter of the house. All of the contaminant leaving the indoor air space is assumed does so via air exchange with the ambient. The indoor control volume is assumed to consist of only of the basement, assumed as having a total volume of 300 m^3. Clearly different assumptions could be made regarding the structural features and the size of the crack entry route, but for present purposes, this is unimportant as the intent is only to show for "typical" values what the influence of certain other features can be. The modeled surrounding soil domain extends 5 meters from the perimeter of the house, and is assumed to consist of sandy clay (except as noted). Directly beneath the foundation slab, there is assumed to be a 30 cm (one foot) thick gravel layer, except in certain cases where this sub-base material is assumed to be the same as the surrounding soil (termed a "uniform" soil scenario). The preferential pathway is modeled as a 10 cm (4") pipe that exits into the gravel sub-base beneath the structure. The air in the pipe is assumed to be contaminated with TCE at a vapor concentration equal to the vapor in equilibrium with the groundwater contaminant concentration below the structure, modified by a scaling factor χ, which is allows the contaminant concentration in the pipe to be parameterized. The groundwater beneath the structure is assumed to be homogeneously contaminated with trichloroethylene (TCE) as a prototypical contaminant. The groundwater itself is not modeled, as the bottom of the model domain is defined by the top of the water table. The ground surface and the pipe are both assumed to be sources of air to the soil domain. Both are assumed to be at reference atmospheric pressure. Vapor transport in the soil is governed by Richard's equation, a modified version of Darcy's Law, taking the variability of soil moisture in the vadose zone into account.[21] The van Genuchten equations are used to predict the soil moisture content and thus the effective permeability of the soil.[22] The effective diffusivity of contaminant in soil is calculated using the Millington-Quirk model.[23] The transport of vapor contaminant in the soil is assumed to be governed by the advection-diffusion equation, in which either advection or diffusion may dominate depending upon position and particular circumstances. The equations and the boundary conditions are given in Table 1.

Drivers For Indoor Air Contaminant Variability

The Role Of Building Depressurization/Pressurization

Out of the factors that influence IACC in VI, pressure is one of the most dynamic ones, and the relationship between changes in indoor/outdoor pressure difference and IACC are examined in Figure 1. Three well-studied VI sites are considered, the "ASU house" near Hill AFB in Utah, a building at North Island NAS in California and a duplex in Indianapolis.

The absolute IACC at these sites vary significantly, therefore some means of comparing them all to each other is necessary. Additionally, the focus in this section is the driver for variations in IACC, and representation of the variations between the different sites must also be achieved, specifically variations on the scale of order of magnitudes is of the greatest interest, as these are the largest hinderance to proper site IACC characterization. To achieve these goals, the log-10 deviation from the mean IACC (μ) within each dataset is calculated, e.g. 10μ indicates the IACC is an order of magnitude above the mean IACC for the dataset. On the y-margin in figures 1a and 1b, the univariate KDE distribution of deviation from the mean may be seen.

The indoor/outdoor pressure differences are simply taken as it, and their univariate KDE distributions are shown on the x-margin. A negative pressure difference indicate that the building is underpressurized relative to outdoor.

The relationship between the deviation from mean IACC, and indoor/outdoor pressure difference may be seen in the central portion of each figure, in the form of a bivariate KDE

Table 1: Governing equations, boundary conditions & model input parameters. (See below for table of nomenclature).

(a) Governing equations

Unsteady-CSTR	$V\frac{du}{dt} = \int_{A_{\text{ck}}} j_{\text{ck}} dA - uA_e V$
Richard's equation	$\nabla \cdot \rho\Big(-\frac{\kappa_s}{\mu} k_r \nabla p\Big) = 0$
Millington-Quirk	$D_{\text{eff}} = D_{\text{air}} \frac{\theta_g^{10/3}}{\theta_t^2} + \frac{D_{\text{water}}}{K_H}\frac{\theta_w^{10/3}}{\theta_t^2}$
Advection-diffusion equation	$\frac{\partial}{\partial t}\Big(\theta_w c_w + \theta_g c\Big) = \nabla(D_{\text{eff}} \cdot \nabla c) - \vec{u} \cdot \nabla c$
van Genuchten equations	$\text{Se} = \frac{\theta_w - \theta_r}{\theta_t - \theta_r} = [1 + \lvert\alpha z\rvert^n]^{-m}$ $\theta_g = \theta_t - \theta_w$ $k_r = (1-\text{Se})^l[1-(\text{Se}^{-m})^m]^2$ $m = 1 - 1/n$

(b) Boundary conditions

Boundary	**Richard's equation**	**Advection-diffusion equation**
At foundation crack	$p = p_{\text{in/out}}$ (Pa)	$j_{\text{ck}} = \frac{uc}{1-\exp(uL_{\text{slab}}/D_{\text{air}})}$
At groundwater source	N/A	$c = c_{\text{gw}} K_H$ (μg/m^3)
At ground surface	$p = 0$ (Pa)	$c = 0$ (μg/m^3)
Exit of preferential pathway	$p = 0$ (Pa)	$c = c_{\text{gw}} K_H \chi$ (μg/m^3)

(c) Soil & gravel properties[24–26]

Soil	Permeability (m^2)	Density (kg/m^3)	θ_s	θ_r	α (1/m)	n
Gravel	$1.3 \cdot 10^{-9}$	1680	0.42	0.005	100	3.1
Sand	$9.9 \cdot 10^{-12}$	1430	0.38	0.053	3.5	3.2
Sandy Clay	$1.7 \cdot 10^{-14}$	1470	0.39	0.12	3.3	1.2

(d) Trichloroethylene (diluted in air) properties[25,26]

D_{air} (m^2/h)	D_{water} (m^2/h)	Density (kg/m^3)	Viscosity (Pa $\cdot$ s)	K_H	M (g/mol)
$2.47 \cdot 10^{-2}$	$3.67 \cdot 10^{-6}$	1.614	$1.86 \cdot 10^{-5}$	0.403	131.39

(e) Building properties

V_{base} (m^3)	L_{slab} (cm)	A_e (1/hr)
300	15	0.5

distribution. The p-value and Pearson's r-value for each bivariate distribution is shown in the legend.

In Figure 1a the North Island and ASU house datasets are plotted, with blue representing

Figure 1: KDE analysis of IACC dependence on indoor/outdoor pressure difference at the ASU house and North Island site (1a) and the Indianapolis site (1b). p-values and Pearson's r-values shown for each dataset.

(a) Period before and after the PP was shut at the ASU house considered separately; North Island dataset considered in its entirety.

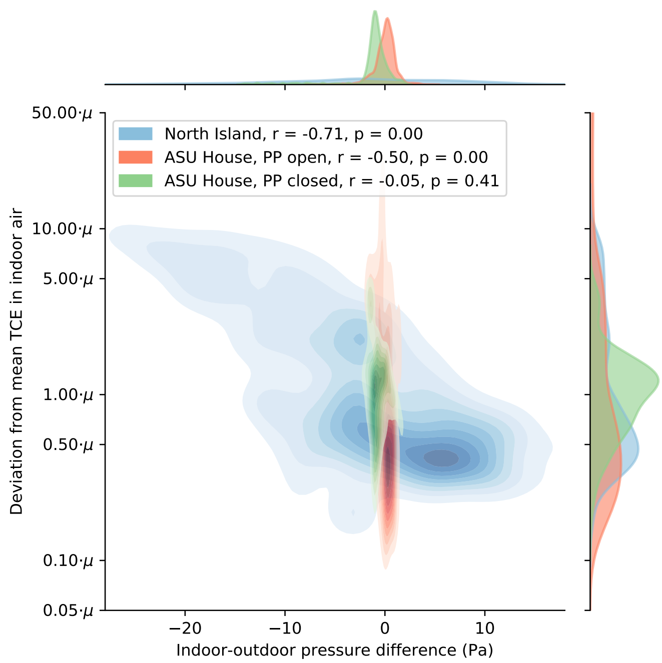

(b) Chloroform and PCE considered separeately at Indianapolis duplex 422.

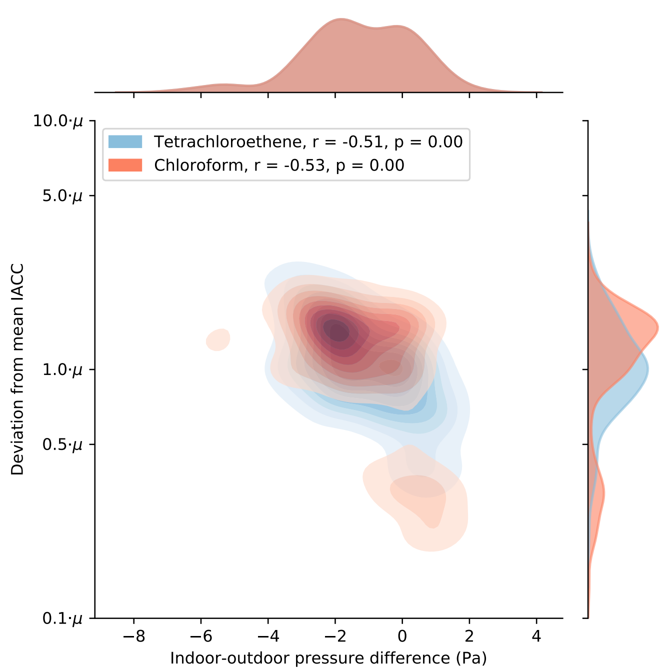

the North Island site, and with red and green representing the ASU house. The ASU house dataset is split into two different parts, the first (red) is data from the time period before the PP was discovered, the second (green) is from after the PP was sealed off. At both of these sites, TCE was the only contaminant considered. The IACC of Chloroform and PCE in the 422 part of the Indianapolis duplex are considered in Figure 1b.

From Figure 1a, it is apparent that the three datasets differ significantly from each other. The North Island site exhibit the greatest variation in both pressure difference and IACC, in fact, looking at the univariate pressure distribution - it is almost entirely flat and spanning from extremly high and low values. A likely explation for this is the poor condition of the structure, rendering it highly susceptible to envivornmental influnces.

To accompany this, there is significant variation in IACC, that has a relativly strong link with pressure difference ($r = -0.71$), although there is clearly a distinct peak (around 0.5μ) that is primally associated with the smaller negative and positive pressure differences ($-4 \leq \Delta p \leq 8$). This demonstrates that at this particular site, the very large variations (an order of magnitude or more) are primarily influenced by the unusually large pressure difference fluctations. Likely, this relationship is amplified by the fact that the soil surrounding the structure is sandy and therefore relatively permeable - increasing the influence of pressure differences. However, despite all this, pressure differences can only partly explain the variations observed at this site.

The two ASU datasets are not only significantly different from the North Island dataset, but also different from each other. Consider the dataset before the PP was discovered (red) and one can see that the IACC varies significantly (from 0.05μ to more than 50μ, albeit rarely.) This is more variation than was observed at North Island, and yet the distribution of pressure differences is narrow, mostly varying by a few Pa around zero (± 2 Pa), and with $r = -0.50$, suggests that pressure difference is not insignificant but still a weak predictor for the variations in IACC.

The picture changes completely after the PP was closed off, where a similar distribution of pressure differences is observed, but with a signficant reduction in IACC variance to around $\pm 0.5\mu$, resembling something of a log-normal distribution. This clearly shows just how much variance the PP at this site contributed with, and how critical it is to assess whether a PP is present at a particular site in general, lest potentially face unacceptable uncertainty in determining the relevant contaminant exposure. It is also clear that in the absence of a PP, the pressure difference becomes even less important, with the p- and r-value indicating that pressure differences are here insignficant in determining variation in IACC. This also suggests that the PP at the ASU house acted not only as a PP for contaminant vapors, but for air in general - allowing the impermeable soil surrounding the house to be circumvented. PPs, and the factors that influnce them will be explored later in this article.

The Indianapolis duplex also featured a PP, but despite this, there is significantly less variance in IACC of both Chloroform and PCE. The exact reason for this is not known, but considering that the PP at the Indianapolis site was a sanitary sewer, and at ASU the PP was a foundation drain system, it is not inconceivable that their dynamics are quite different. Nevertheless, both PCE and Chloroform are more or less log-normally distributed, with (mostly) less than an order of magnitude variance around the mean, indicating that the varation in IACC are species independent.

The pressure difference distribution exhibit some bimodal characteristics, with a larger variation than was observed at the ASU site. This may explain why the r-values for both PCE and Chloroform, $r = -0.51$ and $r = -0.53$ respectively, are so similar to the ASU site before the PP there was closed; the larger pressure differences, which occured more often than ASU, increase contaminant entry rates to the extent that a PP was needed to "achieve" at the ASU site.

All of these data clearly suggest that there is significant variation in IACC that cannot be easily explained by variations in indoor/outdoor pressure difference - even with a PP. It is also clear that PP may contribute with unacceptable levels of variations, and screening for PPs should be part of any site investiation. It may also be prudent, even in the absence of PP, to add around a half to one order of magnitude margin of error to early screening measurements of indoor air. E.g. if a single sample is less than an order of magnitude from some target limit, it may be justified to perform subsequent samples to better assess the relevant exposure. These data also call the role of advection in VI into question, as "normal" pressure difference ranges are such a poor predictor of IACC variation, which is the opposite of what one would expect if advection was a dominant transport mechanism.

The Role Of Air Exchange Rate

Air exchange rate, which measures how often the interior air in a given building is exchanged with exterior air, is the main parameter characterizing contaminant expulsion, and another highly dynamic process. Exploring the impact of fluctuations in air exchange rate is thus also important for the development of sampling strategies. At the ASU house, the contaminant entry rate into the structure (called emission rate in that study) as well as the building air exchange rate were recorded across time. This allows for exploration of the impact that fluctuating air exchange rate has on the final IACC by solving the CST equation, using the recorded contaminant entry rate as one input, and assuming a constant air exchange rate. The rationale is to show the extent of variability in IACC due to factors other than fluctuations in air exchange rates. We have taken this factor out of consideration by assuming a single constant exchange rate, characteristic of the whole period.

In Figure 2a, the measured IACC and air exchange rate across time are shown, with the predicted IACC assuming a constant air exchange rate. The median air exchange rate value for the pre-CPM period was chosen as this seemed to be the most representative value for this time period. From Figure 2a it may be seen quite clearly that for the non-CPM periods, the calculated IACC assuming constant and actual fluctuating exchange rates are quite similar. In other words, in this instance it is unlikely that the variations in IACC were driven by fluctuations in air exchange rate.

This is more clearly shown in Figure 2b, where KDEs of the IACC are constructed

Figure 2: Comparison between the recorded and the calculated TCE in indoor air at the ASU house, assuming constant air exchange rate. 2a shows the TCE in indoor air across time as well as the exchange rate. 2b shows the distribution of these values for three periods.

(a)

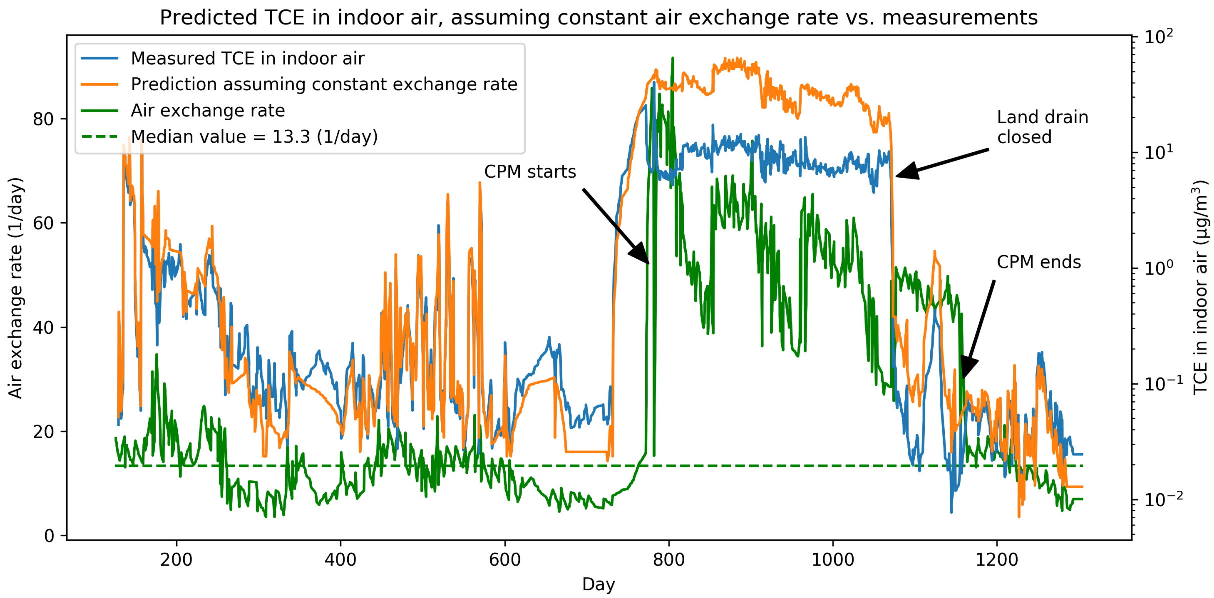

(b)

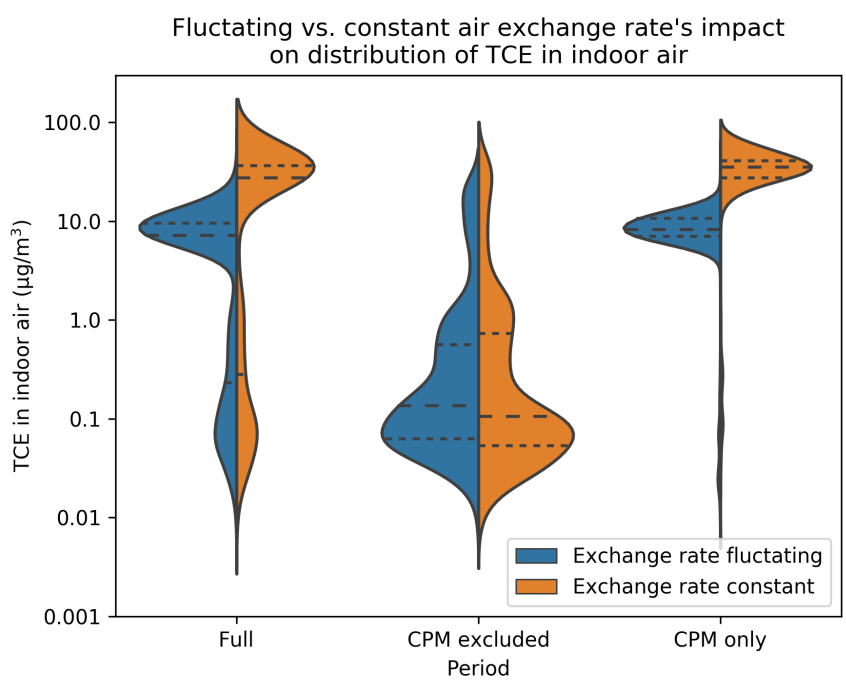

assuming the constant and fluctuating air exchange rate cases. This figure shows the relative probability of being at a particular TCE in indoor air concentration at the ASU house. These are compared to each other for 1. the full measurement period, 2. the non-CPM periods and 3. the CPM period. Looking at the full period, it does not appear as though the two cases of steady and fluctuating air exchange rate are comparable, the distribution functions for IACC are different and offset. The curves to the different sides of the vertical line for the "full" measurement period represent the probability distributions for the indicated values of IACC. It appears as though assuming a constant air exchange rate shifts the IACC probability distribution to higher values. The reason for this are more apparent when considering the CPM and non-CPM periods separately.

Considering only the CPM period, assuming a constant air exchange rate does not influence the shape of the IACC distribution, but assuming constant exchange rate shifts the IACC to a higher values. This is because the actual air exchange rate for this CPM period is significantly higher than the assumed median value, and much more contaminant is actually exchanged with the exterior. The shape of the IACC distribution is not very different from that which takes the air exchange fluctuations into account however, indicating that fluctuating exchange rate is not a major contributor to observed IACC variation for this period (the distinction being drawn between variation and absolute levels of IACC).

The non-CPM period is the condition under which field practitioners would normally collect samples at a VI site. It is clear here that there is only a very minor difference made in assuming a constant vs. real fluctating air exchange rate, again indicating that account for the minor fluctuations of air exchange rate's impact on variations in IACC is not important. Rackes and Waring[27] drew similar conclusions regarding the relationship between IACC and air exchange rate.

The Influence of Preferential Pathways

Conclusions From Steady-State Modeling

Clearly, PPs pose a major problem for site investigations, in particular because they may be difficult or even impossible to anticipate or uncover; even at a well studied site like the

ASU house it took years to discover the PP. Therefore, there is a need to consider other indications that a PP is present.

Figure 3: Attenuation factor relative to contaminant vapor in equilibrium with groundwater as a function of indoor-outdoor pressure difference. The effects of a preferential pathway, that is either contaminated or uncontaminated as well as that of having a gravel sub-base vs. uniform sandy clay soil are considered.

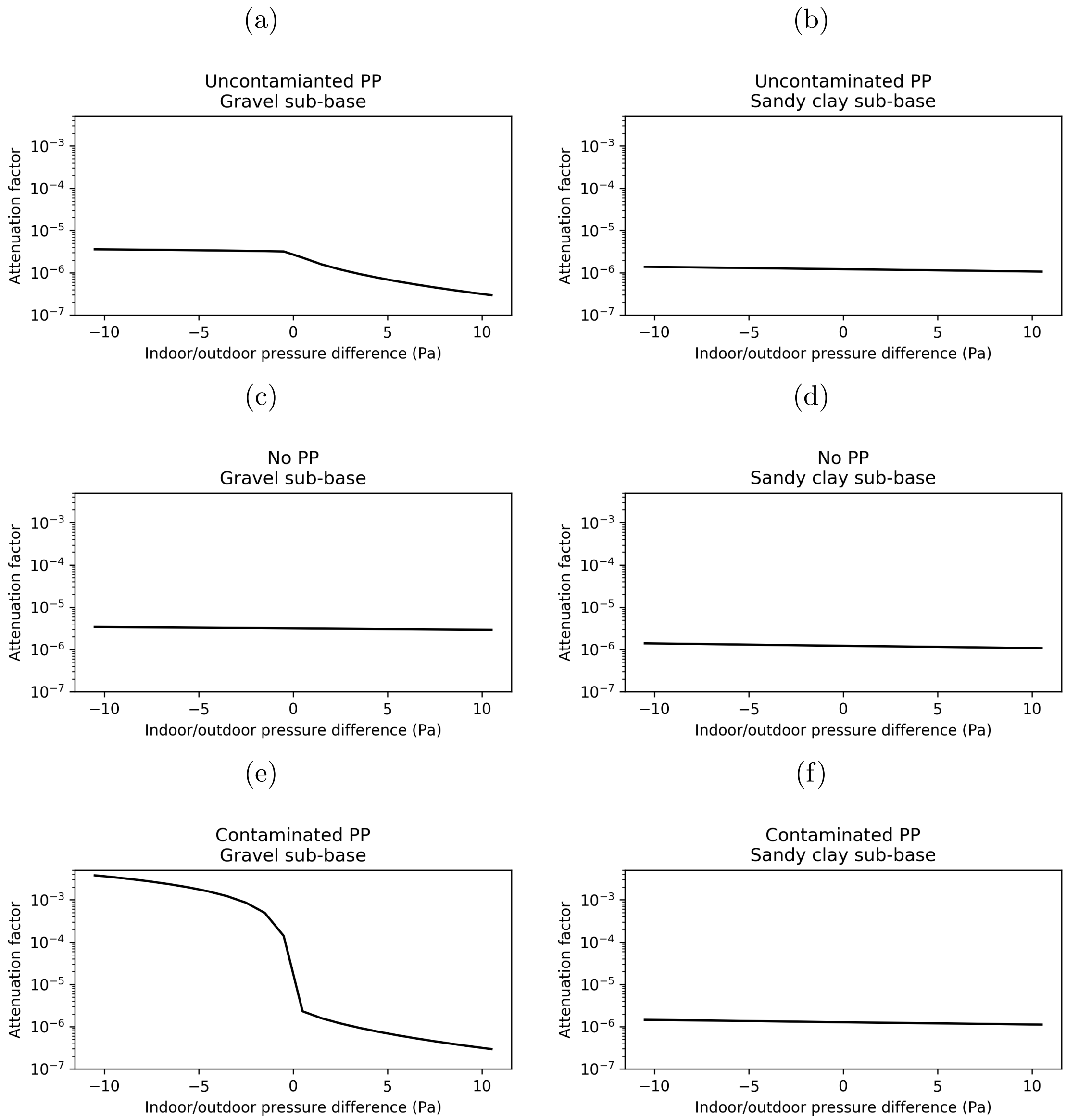

One way has been suggested by the situation at the ASU house, where there clearly was a PP containing contaminant vapor, and the PP exited into a gravel (permeable) sub-base. This situation can be examined using the VI model introduced earlier by examining how IACC is impacted by various factors over a range of indoor-outdoor pressure difference values. Instead of representing IACC as absolute concentration, we now non-dimensionalize with respect to the vapor in equilibrium with the groundwater contaminant concentration. This non-dimensionalized property is commonly called the attenuation factor and is denoted by α_{gw}. The result of a sensitivity analysis relative to several factors is seen in Figure 3. These examine scenarios in which the indoor-outdoor pressure difference is a driver for VI.

In this figure, all the graphs in the left column show results for a scenario, in which the house has a gravel sub-base, with the remaining surrounding soil assumed to be sandy clay. All the right column graphs features only sandy clay soil, directly in contact with the slab. Figure 3a considers an uncontaminated PP ($\chi = 0$), i.e. the PP delivers clean air to beneath the slab. In 3b there is no PP present at all, giving a reference state for a "normal" VI scenario. 3c features a contaminated PP ($\chi = 1$), i.e. the PP delivers contaminant vapor at a concentration characteristic of underlying groundwater.

In terms of conditions that may lead to significant temporal transients in α_{gw}, driven by indoor-outdoor pressure difference, most of the cases in this analysis show negative results. There are only two combinations of factors where significant changes in α_{gw} accompany the changes in indoor-outdoor pressure difference, both involving the permeable (gravel) sub-base into which a PP enters. In 3c, the PP is filled with contaminant vapor whereas figure 3 involves the PP only delivering "clean" air to the gravel sub-base. When the building is overpressurized (positive indoor-outdoor pressure difference), the two cases exhibit similar behavior, i.e. α_{gw} is low as expected.

When the building is underpressurized, the uncontaminated PP case involves barely any increase in α_{gw} while there is a very significant increase in α_{gw} in the contaminated PP case. For the contaminated PP scenario, this is quite easy to understand, as the extra air flow provided by the PP into the gravel sub-base very effectively disperses contaminant vapor across the sub-base and the contaminant entry rate is increased.

When the PP is provides clean air, the increase in air flow into the sub-base with depressurization is the same. However, the resulting increase in air entry rate does not bring in more contaminant as clean air is being drawn in. This means that most of the contaminant entry rate is still only controlled by the usual process of diffusion through the soil, giving a result that is actually similar to that for the "no PP and with gravel sub-base" scenario. Thus, for a PP to be a significant contributor to contaminant entry at a VI site the conditions such as featured in the bottom left case are required, i.e. a permeable sub-base and the PP must be a source of contaminant.

Various techniques for determining the potential for sewer gas entry into a house are described by Nielsen and Hvidberg.[28] Collecting contaminant vapor samples from nearby manholes is also recommended, however one should be aware that contaminant vapors can potentially travel very long distances in a sewer system.[11,13,14]

Figure 4: Attenuation factor vs. indoor-outdoor pressure difference when considering VI scenarios similar to the ASU house and the North Island NAS site (4a and 4b respectively).

(a) (b)

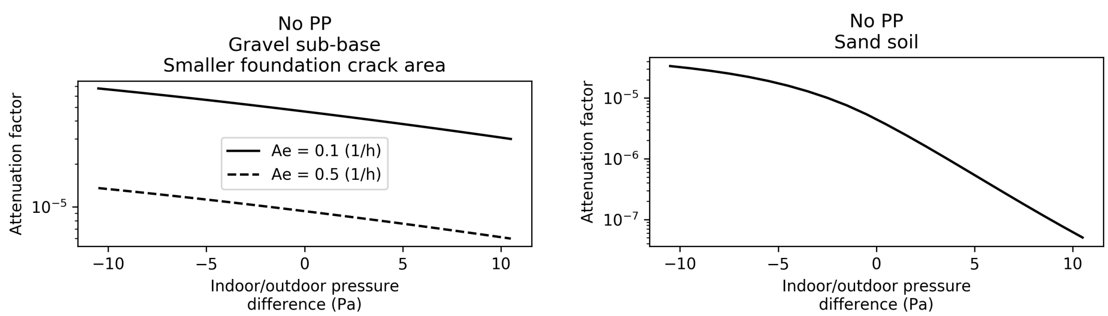

At the ASU house, after the PP was closed, there was still roughly an order of magnitude variation in IACC, the reasons for which Figure 3 does not address. Likewise, there was more than two orders of magnitude observed at the North Island site over the indoor-outdoor pressure difference ranges simulated despite there not being a PP present. Therefore, it is of interest to examine these sites a bit further using the model.

The foundation crack at the ASU house seems by all accounts to be quite small, roughly 180x1 cm and located close to the PP.[9] This crack is smaller than the one assumed in the model used in Figure 3. The influence of indoor-outdoor pressure difference is explored for a case in which a smaller crack area is assumed. We also consider the effects of having a significantly lower air exchange rate, 0.1 vs. the regular 0.5 per hour.

The results of the case shown in Figure 3c is shown in Figure 4a. Even though there is an increase in α_{gw} with increased underpressurization, it is no where near the roughly one order of magnitude recorded at the ASU house after the PP was closed. So while crack dimensions can clearly influence α_{gw}, they cannot be used to infer a bigger role for pressure difference in temporal variations in α_{gw} or IACC. The influence of air exchange rate on α_{gw} predictions is also shown in Figure 4. Clearly, the value of air exchange rate at steady-state conditions will only influence absolute concentrations in the structure. Ultimately, the reason for the transient variability in IACC during the post-CPM period at the ASU house remains elusive, as a Pearson's r analysis between IACC and various factors do not yield any explanation.

In the case of the North Island site, variations in IACC are clearly not related to the existence of a PP. The soil underlying the North Island site is more sand-like.[5] The significance of this is that sand soil is much more permeable than sandy clay soil, which means that α_{gw} will be much more sensitive to changes in indoor-outdoor pressure difference. Thus, another "normal" VI scenario was run but this time with sand soil instead of sandy clay, the results of which may be seen in Figure 4b. Under these conditions, α_{gw} changes significantly with pressurization, spanning roughly two orders of magnitude. This is consistent with what was observed at North Island, as there the span of IACC values was roughly the same across this range of indoor-outdoor pressure difference values. This simulation, together with the Pearson $r = -0.64$ for North Island in Figure 1a suggest that under conditions where the soil around a structure is relatively permeable, indoor-outdoor pressure difference can be a significant driving forces for transient changes in IACC. Therefore, recording the indoor-outdoor pressure difference at a site (in particular if the soil is permeable) may offer insight into the potential for transient changes in IACC (some good methods for doing this are suggested by Nielsen and Hvidberg[28]).

Transient Modeling

Analyzing the impact of a PP using steady-state simulations such as those in Figures 3 and does not revealing about how quickly IACC can change in the presence of a PP. A transient simulation of a VI scenario that is characterized by a PP has been performed, where only the indoor-outdoor pressure difference was temporally changed. The pressure difference is changed in a sinusoidal fashion, defined by (1),

$$p_{\mathrm{in/out}} = 10 \sin\left(2\pi t\right) - 0.5 \tag{1}$$

where t is given in days and $p_{\mathrm{in/out}}$ is the indoor-outdoor pressure difference in Pa. Figure 5 shows the results of this simulation.

Figure 5a shows the IACC response, given as attenuation factor relative to contaminant vapor in equilibrium with groundwater, and the indoor-outdoor pressure difference with time. What is apparent is that α_{gw} closely follows the indoor-outdoor pressure difference, with the max./min. α_{gw} being reached roughly 0.5 hours after the indoor-outdoor pressure difference reaches its max./min.. The reader should be aware that the assumption that the indoor air space can be modeled as a CST overestimates how dynamic this process is as a real house probably would not be perfectly mixed on as a short time scale as this. Regardless, this suggests that VI sites characterized by PPs are highly dynamic and IACC's may change quickly in response to changing indoor-outdoor pressure differences, consistent with what was observed at the ASU house.[3] Again, the dynamics of the indoor-outdoor pressure difference at a VI site can offer insight into the potential for transient behavior of IACC.

Figures 5b and 5c show the contaminant concentration (normalized to the contaminant vapor in equilibrium with groundwater) in the soil and gravel sub-base at three different depths at times of 30 and 42 hr respectively corresponding to roughly the maximum in overpressurization and depressurization respectively. The top layer is 3 m above groundwater and immediately under the house foundation (indicated by the black square). The middle

Figure 5: Transient response of TCE in indoor air (as attenuation factor) and in the surrounding soil & gravel sub-base for a PP VI scenario subject to sinusoidal indoor-outdoor pressure fluctuations. 5a shows the attenuation factor and indoor-outdoor pressure across time. Figures 5b & 5c show the contaminant concentration (normalized to the contaminant vapor in equilibrium with groundwater) in the surrounding soil & gravel sub-base at different depths and times.

(a)

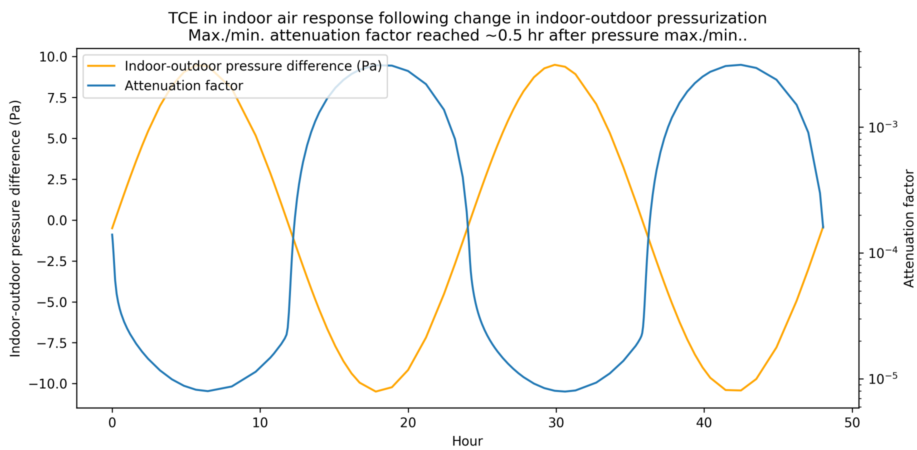

(b) t = 30 hr

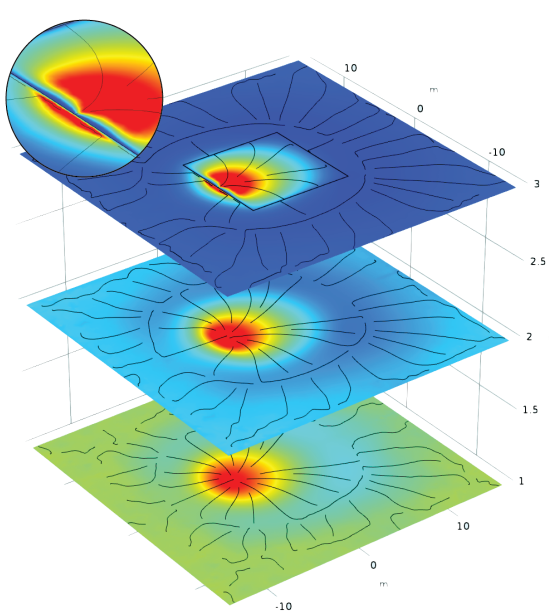

(c) t = 42 hr

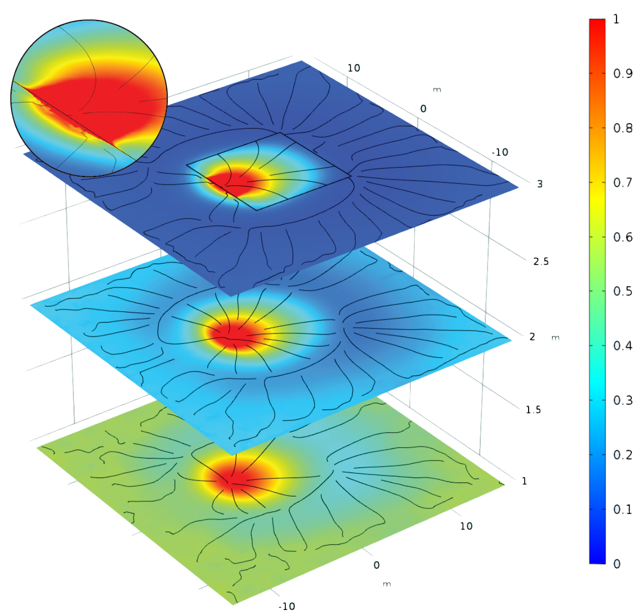

and bottom layers are 2 and 1 m above groundwater respectively. The black streamlines show the contaminant transport flow paths. The region closest to the PP is expanded in the circular insets.

The impact of the PP on the contaminant vapor concentration in the subsurface is apparent in these figures, as one easily sees how (especially) the gravel sub-base is filled up. The contaminant vapor concentration is the highest closest to the PP (which is located at the edge of the gravel sub-base) and decreases with increased distance from the PP. Note that a very small amount of contaminant vapor leaves the gravel sub-base, as the sandy clay has a relatively large resistance to transport compared with gravel. This makes it difficult to detect the contribution of the PP outside the foundation footprint. However, this may not always be true, as vapor contaminant from the PP would disperse more easily into more permeable soils.

It should also be noted that the vapor contaminant emanating from the PP in this model is relatively high concentration; the vapor contaminant concentration is equal to that in equilibrium with the groundwater source. This does not always seem to be the case, as VI sites that have uncovered PPs find that the vapor contaminant emanating from the PP can be lower than that.[9] Therefore, it may be much more difficult than it may appear in Figures 5b and 5c to localize a vapor contaminant hotspot as a way to determining the presence of a PP at a particular VI site.

The insert circles in figures 5b and 5c also show that for the simulated time period, only a small amount of the contaminant enters the structure (as evident by the blue low concentration zone around the perimeter), yet a very large increase in α_{gw} occurs. The concentration in the rest of the sub-base is unchanged. This suggests that once a PP has deposited contaminant underneath a structure, it may persist for a long time period, as pointed out by Guo.[9]

Acknowledgement

This project was supported by grant ES-201502 from the Strategic Environmental Research and Development Program and Environmental Security Technology Certification Program (SERDP-ESTCP).

Table 2: Abbreviations & symbols

Abbreviation or symbol	**Explanation**
VI	Vapor intrusion
PP	Preferential pathway
L_{slab}	Thickness of the foundation concrete slab
p	Pressure
u	TCE in indoor air concentration
c	TCE in soil gas concentration
D_{air}	Diffusion of TCE in air
D_{water}	Diffusion of TCE in water
D_{eff}	Effective Diffusion of TCE in soil
K_H	Henry's Law constant
θ_g, θ_w & θ_s	Vapor, water filled & saturated soil porosity
θ_r	Residual moisture porosity
$\alpha,\ l,\ n$ & m	van Genuchten parameters
Se	Soil moisture saturation
k_r	Relative permeability
α_{gw}	Attenuation factor

References

(1) U.S. Environmental Protection Agency, OSWER Technical Guide for Assessing and Mitigating the Vapor Intrusion Pathway From Subsurface Vapor Sources To Indoor Air. `https://www.epa.gov/sites/production/files/2015-09/documents/oswer-vapor-intrusion-technical-guide-final.pdf`, 00005.

(2) Folkes, D.; Wertz, W.; Kurtz, J.; Kuehster, T. Observed Spatial and Temporal Distributions of CVOCs at Colorado and New York Vapor Intrusion Sites. *29*, 70–80, 00048.

(3) Holton, C.; Luo, H.; Dahlen, P.; Gorder, K.; Dettenmaier, E.; Johnson, P. C. Temporal

Variability of Indoor Air Concentrations under Natural Conditions in a House Overlying a Dilute Chlorinated Solvent Groundwater Plume. *47*, 13347–13354, 00028.

(4) Johnston, J. E.; Gibson, J. M. Spatiotemporal Variability of Tetrachloroethylene in Residential Indoor Air Due to Vapor Intrusion: A Longitudinal, Community-Based Study. *24*, 564, 00018.

(5) Hosangadi, V.; Shaver, B.; Hartman, B.; Pound, M.; Kram, M. L.; Frescura, C. High-Frequency Continuous Monitoring to Track Vapor Intrusion Resulting From Naturally Occurring Pressure Dynamics. *27*, 9–25, 00001.

(6) McHugh, T.; Loll, P.; Eklund, B. Recent Advances in Vapor Intrusion Site Investigations. *204*, 783–792, 00005.

(7) Johnson, P. C.; Holton, C. W.; Guo, Y.; Dahlen, P.; Luo, E. H.; Gorder, K.; Dettenmaier, E.; Hinchee, R. E. Integrated Field-Scale, Lab-Scale, and Modeling Studies for Improving Our Ability to Assess the Groundwater to Indoor Air Pathway at Chlorinated Solvent-Impacted Groundwater Sites. 00003.

(8) Holton, C. W. Evaluation of Vapor Intrusion Pathway Assessment Through Long-Term Monitoring Studies. `https://repository.asu.edu/attachments/150778/content/Holton_asu_0010E_15040.pdf`, 00003.

(9) Guo, Y. Vapor Intrusion at a Site with an Alternative Pathway and a Fluctuating Groundwater Table. `https://repository.asu.edu/items/36435`, 00001.

(10) Guo, Y.; Holton, C.; Luo, H.; Dahlen, P.; Gorder, K.; Dettenmaier, E.; Johnson, P. C. Identification of Alternative Vapor Intrusion Pathways Using Controlled Pressure Testing, Soil Gas Monitoring, and Screening Model Calculations. *49*, 13472–13482, 00019.

(11) McHugh, T.; Beckley, L.; Sullivan, T.; Lutes, C.; Truesdale, R.; Uppencamp, R.;

Cosky, B.; Zimmerman, J.; Schumacher, B. Evidence of a Sewer Vapor Transport Pathway at the USEPA Vapor Intrusion Research Duplex. *598*, 772–779, 00007.

(12) Pennell, K. G.; Scammell, M. K.; McClean, M. D.; Ames, J.; Weldon, B.; Friguglietti, L.; Suuberg, E. M.; Shen, R.; Indeglia, P. A.; Heiger-Bernays, W. J. Sewer Gas: An Indoor Air Source of PCE to Consider During Vapor Intrusion Investigations. *33*, 119–126, 00022.

(13) Roghani, M.; Jacobs, O. P.; Miller, A.; Willett, E. J.; Jacobs, J. A.; Viteri, C. R.; Shirazi, E.; Pennell, K. G. Occurrence of Chlorinated Volatile Organic Compounds (VOCs) in a Sanitary Sewer System: Implications for Assessing Vapor Intrusion Alternative Pathways. *616-617*, 1149–1162, 00001.

(14) Riis, C. E.; Christensen, A. G.; Hansen, M. H.; Husum, H.; Terkelsen, M. Vapor Intrusion through Sewer Systems: Migration Pathways of Chlorinated Solvents from Groundwater to Indoor Air. Seventh International Conference on Remediation of Chlorinated and Recalcitrant Compounds. 00012.

(15) Brenner, D. Results of a Long-Term Study of Vapor Intrusion at Four Large Buildings at the NASA Ames Research Center. *60*, 747–758, 00003.

(16) U.S. Environmental Protection Agency, Assessment of Mitigation Systems on Vapor Intrusion: Temporal Trends, Attenuation Factors, and Contaminant Migration Routes under Mitigated And Non-Mitigated Conditions. 00002.

(17) McHugh, T. E.; Beckley, L.; Bailey, D.; Gorder, K.; Dettenmaier, E.; Rivera-Duarte, I.; Brock, S.; MacGregor, I. C. Evaluation of Vapor Intrusion Using Controlled Building Pressure. *46*, 4792–4799, 00037.

(18) Shen, R.; Pennell, K. G.; Suuberg, E. M. Influence of Soil Moisture on Soil Gas Vapor Concentration for Vapor Intrusion. *30*, 628–637, 00015 WOS:000325689400005.

(19) Yao, Y.; Wang, Y.; Zhong, Z.; Tang, M.; Suuberg, E. M. Investigating the Role of Soil Texture in Vapor Intrusion from Groundwater Sources. *46*, 776–784, 00003.

(20) Yao, Y.; Mao, F.; Ma, S.; Yao, Y.; Suuberg, E. M.; Tang, X. Three-Dimensional Simulation of Land Drains as a Preferential Pathway for Vapor Intrusion into Buildings. *46*, 1424–1433, 00002.

(21) Richards, L. A. Capillary Conduction of Liquids through Porous Mediums. *1*, 318–333, 05183.

(22) van Genuchten, M. T. A Closed-Form Equation for Predicting the Hydraulic Conductivity of Unsaturated Soils. *44*, 892–898, 00004.

(23) Millington, R. J.; Quirk, J. P. Permeability of Porous Solids. *57*, 1200, 01813.

(24) Dan, H.-C.; Xin, P.; Li, L.; Li, L.; Lockington, D. Capillary Effect on Flow in the Drainage Layer of Highway Pavement. *39*, 654–666, 00007.

(25) Abreu, L. D. V.; Schuver, H. Conceptual Model Scenarios for the Vapor Intrusion Pathway. `https://www.epa.gov/sites/production/files/2015-09/documents/vi-cms-v11final-2-24-2012.pdf`, 00010.

(26) U.S. Environmental Protection Agency, Users's Guide For Evaluating Subsurface Vapor Intrusion Into Buildings. `https://www.epa.gov/sites/production/files/2015-09/documents/2004_0222_3phase_users_guide.pdf`, 00000.

(27) Rackes, A.; Waring, M. S. Do Time-Averaged, Whole-Building, Effective Volatile Organic Compound (VOC) Emissions Depend on the Air Exchange Rate? A Statistical Analysis of Trends for 46 VOCs in U.S. Offices. *26*, 642–659, 00000.

(28) Nielsen, K. B.; Hvidberg, B. Remediation Techniques for Mitigating Vapor Intrusion from Sewer Systems to Indoor Air. *27*, 67–73, 00002.